VOLUME 120, NUMBER 7
FEBRUARY 25, 1998

JOURNAL OF THE AMERICAN CHEMICAL SOCIETY

A Solid-State Nitrogen-15 Nuclear Magnetic Resonance Spectroscopic and Quantum Chemical Investigation of Nitrosoarene−Metal Interactions in Model Systems and in Heme Proteins

Renzo Salzmann,[†] Mark Wojdelski,[‡] Michael McMahon,[§] Robert H. Havlin,[⊥] and Eric Oldfield*

Contribution from the Department of Chemistry, University of Illinois at Urbana-Champaign, 600 South Mathews Avenue, Urbana, Illinois 61801

Received May 16, 1997. Revised Manuscript Received October 31, 1997

Abstract: We have obtained the solid-state ^{15}N nuclear magnetic resonance isotropic chemical shifts and/or shielding tensor elements for a range of nitrosoarene complexes: *p*-[^{15}N]nitroso-*N*,*N*-dimethylaniline, *p*-[^{15}N]-nitroso-*N*,*N*-dimethylaniline hydrochloride monohydrate, $PdCl_2$(*p*-[^{15}N]nitroso-*N*,*N*-dimethylaniline)$_2$, $ZnCl_2$-(*p*-[^{15}N]nitroso-*N*,*N*-dimethylaniline)$_2$, $SnCl_2(CH_3)_2$(*p*-[^{15}N]nitroso-*N*,*N*-dimethylaniline)$_2$, $PdCl_2$([^{15}N]-nitrosobenzene)$_2$, [$Fe(CO)_3$([^{15}N]nitrosobenzene)]$_2$, and the [^{15}N]nitrosobenzene adducts of horse heart myoglobin and adult human hemoglobin. The isotropic chemical shifts range from 171 to 802 ppm downfield from $NH_{3(ext,l)}$. Using a density functional method, we have computed the isotropic shifts, the shielding tensor elements, and the absolute shieldings, for each of these compounds. There is excellent accord between theory and experiment. In addition, the orientations of the tensors have been calculated, and for the dimer of PhNO, *cis*-dioxyazodibenzene, there is good accord with an experimental determination of the shielding tensor. Our results indicate that the shielding patterns observed from compound to compound are overwhelmingly dominated by the behavior of σ_{11}, the least shielded element of the shielding tensor, which is oriented close to the N−O bond vector (perpendicular to the PhNO π orbital). We also find an excellent correlation between σ_{11} and the N−O Mayer bond order, with hemoglobin, myoglobin and all model compounds fitting the correlation well ($R^2 = 0.963$). The nitrosoarenes have among the largest known ^{15}N shielding tensor widths, but by using density functional methods, it is possible to accurately compute them, even when they are bonded to transition metals. Overall, these results thus represent the first comprehensive NMR and quantum chemical study of RNO bonding to heme proteins and model systems, and should form the basis for future comparative studies of the biologically important isoelectronic species, dioxygen.

Introduction

The topic of ligand binding to metal sites in metalloproteins has been of great interest for many years.[1−3] Of particular note has been the topic of CO and O_2 binding to hemoglobin (Hb) and myoglobin (Mb), since CO/O_2 discrimination is critical from the standpoint of Hb/Mb structure−function.[4] Of the two ligands, most studies have focused on CO, in large part because of the stability and spectroscopic accessibility, via infrared and Raman studies, of CO−heme and CO−heme protein complexes.[5−7] However, it is clearly desirable in order to more fully understand the nature of metal−ligand bonding to develop and apply new experimental and theoretical methods, since, for

[†] Swiss National Science Foundation Postdoctoral Fellow, 1996−1997; American Heart Association, Inc., Illinois Affiliate, Postdoctoral Fellow, 1997−1998.

[‡] Colgate-Palmolive Scholar.

[§] National Institutes of Health Cellular and Molecular Biophysics Training Grant Trainee (Grant GM-08276).

[⊥] Barry Goldwater Fellow. Present address: Department of Chemistry, University of California, Berkeley, CA 94720.

S0002-7863(97)01587-4 CCC: $15.00
Published on Web 02/05/1998

example, even the assignment of metal−ligand vibrational spectra appears somewhat controversial.[8,9] One approach is to develop and apply spectroscopic methods in which peak assignments are unambiguous, and in which the spectroscopic observables can be evaluated using first principles methods. For example, the ^{57}Fe Mössbauer electric field gradient (efg) can, at least in principle, give unique structural information,[10] but has not yet been fully analyzed theoretically because of the difficulties associated with very large basis set calculations, together with the likely need to include the effects of electron correlation in the calculations. A second approach might involve studies of ^{57}Fe nuclear magnetic resonance chemical shielding[11−14] as well as ligand shielding and efgs,[15] using ^{13}C- and ^{17}O-labeled compounds, and a third basic approach involves the study of ligands whose structures are isoelectronic with CO and O_2. For example, the alkyl isocyanides (RNC) are isoelectronic with CO,[2,3] and are expected to bond in a very similar manner, but have variable R groups, which can be used to help probe the ligand binding site in Hb and Mb.[16,17] Similarly, nitroso compounds, RNO (R = aliphatic or aromatic), are isoelectronic with O_2 (HNO ≡ O_2) and, based on X-ray crystallographic studies of leghemoglobin[18] and model porphyrins,[19] as well as in part on the results of Mössbauer spectroscopy,[20] appear to bind to Fe in heme proteins in a manner similar to that of dioxygen. They also have variable R groups, like the isocyanides, enabling in principle a mapping of heme pocket dynamics. Indeed, nitroso compounds bind exceptionally strongly to heme proteins, displacing even CO. Warburg et al.,[21] Jung,[22] and Keilin and Hartree[23] all pursued this topic half a century ago and concluded that aromatic nitroso compounds (formed via ferric iron oxidation of phenylhydroxylamines) bound very tightly to Hb and Mb. In a similar vein, Mansuy et al.[24,25] have investigated the binding of aliphatic nitroso compounds to cytochrome P_{450}, and have attributed a number of pharmacological/toxicological properties of drugs, such as amphetamines, to their degradation to aliphatic nitroso compounds, which bind strongly to cytochromes P_{450}.

In this study, we present initial results on metal−nitrosoarene bonding in a series of generally well-characterized model compounds, as well as initial experimental and theoretical studies of heme−nitrosobenzene bonding in hemoglobin and myoglobin. We focus primarily on solid-state ^{15}N NMR studies of ^{15}N-labeled nitrosoarenes, both free and bonded to different metals, since this provides a large database with which to test the accuracy of the theoretical predictions. For example, in previous work it has been shown that *p*-$NMe_2C_6H_4{}^{15}NO$, *p*-[^{15}N]-nitroso-*N*,*N*-dimethylaniline (NODMA), has one of the largest ^{15}N chemical shift anisotropies known.[26] It serves therefore as a stringent test for chemical shift (shielding) calculations because its shielding is so unusual. Moreover, it and the related PhNO bind strongly to many metal ions, providing a wide variety of structural environments and shift tensors in systems having, for the most part, accurate crystal structures. This enables, again in principle, the accurate prediction of numerous ^{15}N chemical shielding tensor elements, their orientations, and a comparison between theory and experiment. Once success has been demonstrated with these well-characterized systems, then the more complex heme−ligand (protein) systems can be investigated with some confidence in the accuracy of the results obtained.

There have been many possible structure types proposed for nitrosoarene−metal (RNO−M) complexes.[27] The most common among these are monodentate N-bonding, monodentate O-bonding, and bidentate coordination by both nitrogen and oxygen to one or two metals.[27−30] We have chosen a selection of the more common monodentate N-bonding systems, which might reasonably be expected to resemble the heme bonding situation,[18,19] together with the more unusual bridged dimer species, $(PhNO)_2Fe_2(CO)_4$,[27] and one O-bonded species. O-bonding has only been found for *p*-nitroso-*N*,*N*-dimethylaniline, **1**, and nitrosodicyanomethanide Fe(TPP){η-ONC(CN)$_2$}.[28−32] The O-bonding of *p*-nitroso-*N*,*N*-dimethylaniline is presumably favored by the quinonoid structure **1a** of **1**, the enhanced basicity of the O^- site favoring metal−oxygen coordination.[33,34] The

(1) Pauling, L.; Coryell, C. D. *Proc. Natl. Acad. Sci. U.S.A.* **1936**, *22*, 210−216.
(2) Pauling, L. *Nature* **1964**, *203*, 182−183.
(3) Antonini, E.; Brunori, M. *Hemoglobin and Myoglobin in Their Reactions with Ligands*; North-Holland Publishing Co: Amsterdam, London, 1971.
(4) Springer, B. A.; Sligar, S. G.; Olson, J. S.; Phillips, G. N., Jr. *Chem. Rev. (Washington, D.C.)* **1994**, *94*, 699−714.
(5) Li, X. Y.; Spiro, T. G. *J. Am. Chem. Soc.* **1988**, *110*, 6024−6033.
(6) Ray, G. B.; Li, S. Y.; Ibers, J. A.; Sessler, J. L.; Spiro, T. G. *J. Am. Chem. Soc.* **1994**, *116*, 162−176.
(7) Lim, M.; Jackson, T. A.; Anfinrud, P. A. *Science* **1995**, *269*, 962−965.
(8) Maxwell, J. C.; Volpe, J. A.; Barlow, C. H.; Caughey, W. S. *Biochem. Biophys. Res. Commun.* **1974**, *58*, 166−171. Barlow, C. H.; Maxwell, J. C.; Wallace, W. J.; Caughey, W. S. *Biochem. Biophys. Res. Commun.* **1973**, *55*, 91−95.
(9) Potter, W. T.; Tucker, M. P.; Houtchens, R. A.; Caughey, W. S. *Biochemistry* **1987**, *26*, 4699−4707. Miller, L. M.; Chance, M. R. *J. Am. Chem. Soc.* **1994**, *116*, 9662−9669. Hirota, S.; Ogura, T.; Kitagawa, T. *J. Am. Chem. Soc.* **1995**, *117*, 821−822.
(10) Case, D. A.; Huynh, B. H.; Karplus, M. *J. Am. Chem. Soc.* **1979**, *101*, 4433−4453.
(11) Baltzer, L.; Becker, E. D.; Averill, B. A.; Hutchinson, J. M.; Gansow, O. A. *J. Am. Chem. Soc.* **1984**, *106*, 2444−2446.
(12) Lee, H. C.; Gard, J. K.; Brown, T. L.; Oldfield, E. *J. Am. Chem. Soc.* **1985**, *107*, 4087−4088.
(13) Chung, J.; Lee, H. C.; Oldfield, E. *J. Magn. Reson.* **1990**, *90*, 148−157.
(14) Mink, L. M.; Polam, J. R.; Christensen, K. A.; Bruck, M. A.; Walker, F. A. *J. Am. Chem. Soc.* **1995**, *117*, 9329−9339.
(15) Park, K. D.; Guo, K.; Adebodun, F.; Chiu, M. L.; Sligar, S. G.; Oldfield, E. *Biochemistry* **1991**, *30*, 2333−2347.
(16) Mims, M. P.; Olson, J. S.; Russu, I. M.; Miura, S.; Cedel, T. E.; Ho, C. *J. Biol. Chem.* **1983**, *258*, 6125−6134.
(17) Johnson, K. A. High-Resolution X.-Ray Structures of Myoglobin and Hemoglobin-Alkyl Isocyanide Complexes. Ph.D. Thesis, Rice University, 1993.
(18) Arstyunyan, E. G.; Kuranova, I. P.; Uainstein, B. K.; Steigemann, W. *Kristallografiya* **1980**, *25*, 80−81.
(19) Mansuy, O.; Battioni, P.; Chottard, J.-C.; Riche, C.; Chiaroni, A. *J. Am. Chem. Soc.* **1983**, *105*, 455−463.
(20) Gang, P.; Regnard, J. R.; Battioni, P.; Mansuy, D. *Chem. Phys.* **1980**, *45*, 401−408.
(21) Wärburg, O.; Kubowitz, T.; Christian, W. *Biochem. Z.* **1931**, *242*, 170−205.
(22) Jung, F. *Naturwissenschaften* **1940**, *28*, 264−265.
(23) Keilin, D.; Hartree, E. F. *Nature* **1943**, *151*, 390−391.
(24) Mansuy, D.; Gans, P.; Chottard, J.-C.; Bartoli, J.-F. *Eur. J. Biochem.* **1977**, *76*, 607−615. Mansuy, D.; Beaune, P.; Cresteil, T.; Bacot, C.; Chottard, J.-C.; Gans, P. *Eur. J. Biochem.* **1979**, 573−579.
(25) Mansuy, D. *Biochimie* **1978**, *60*, 969−977.
(26) Lumsden, M. D.; Wu, G.; Wasylishen, R. E.; Curtis, R. O. *J. Am. Chem. Soc.* **1993**, *115*, 2825−2832.
(27) Cameron, M.; Gowenlock, B. G.; Parish, R. V.; Vasapollo, G. *J. Organomet. Chem.* **1994**, *482*, 227−230.
(28) Bohle, D. S.; Conklin, B. J.; Hans, C.-H. *Inorg. Chem.* **1995**, *34*, 2569−2581.
(29) Koerner von Gustorf, F.; Henry, M. C.; Sacher, R. E.; Di Pietro, C. *Z. Naturforsch. B* **1966**, *21*, 1152−1158.
(30) Liebeskind, L. S.; Sharpless, B. K., Wilson, R. D.; Ibers, J. A. *J. Am. Chem. Soc.* **1978**, *100*, 7061−7063.
(31) Little, R. G.; Doedens, R. J. *Inorg. Chem.* **1973**, *12*, 537−540.
(32) Cameron, M.; Gowenlock, B. G.; Vasapollo, G. *J. Organomet. Chem.* **1991**, *403*, 325−333.
(33) MacNicol, D. D.; Wallace, R.; Brand, J. C. D. *Trans. Faraday Soc.* **1965**, *61*, 1−4.
(34) Rømming, C.; Talberg, H. J. *Acta Chem. Scand.* **1973**, *27*, 2246−2248.

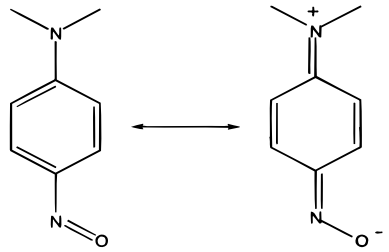

1 **1a**

major contribution of the polar resonance form **1a** is evidenced by the large dipole moment of 6.90 D,[35] to be compared with only 3.14 D in nitrosobenzene itself.[36]

Unfortunately, there is some uncertainty as to the fundamental vibrational frequency of the NO group in such complexes, with values of either 1500 or 1370 cm^{-1} being reported.[37,38] This often makes it difficult to ascertain, independent of X-ray results, whether N or O coordination is involved. Similarly, in the hydrochloride salt of **1**, it is difficult to ascertain from IR spectroscopy alone the protonation site (Me_2N or NO). However, with solid-state NMR, such assignment difficulties can be circumvented by the use of specifically ^{15}N-labeled materials, and as we show below, by using a combination of solid-state NMR and quantum chemistry, it is possible to make a detailed study of metal− or hydrogen−ligand interactions in each system, as well as permit an initial investigation of metal−ligand interactions in the much larger systems, myoglobin and hemoglobin, where the RNO ligand acts as an isoelectronic probe of $Fe-O_2$ bonding.

Experimental Section

Synthetic Aspects. *p*-[^{15}N]Nitroso-*N*,*N*-dimethylaniline hydrochloride monohydrate, *p*-[^{15}N]nitroso-*N*,*N*-dimethylaniline,[39] $PdCl_2$(*p*-[^{15}N]nitroso-*N*,*N*-dimethylaniline)$_2$,[35] $ZnCl_2$(*p*-[^{15}N]nitroso-*N*,*N*-dimethylaniline)$_2$,[40] $SnCl_2(CH_3)_2$(*p*-[^{15}N]nitroso-*N*,*N*-dimethylaniline)$_2$,[41] and $PdCl_2$([^{15}N]nitrosobenzene)$_2$[42−44] were synthesized according to standard literature procedures using ^{15}N-labeled $PhNO_2$ or $NaNO_2$ (Cambridge Isotopes) as ^{15}N sources.

$[Fe(CO)_3$([^{15}N]nitrosobenzene)$]_2$. We used the following modifications to the published procedure.[45] To 9 mL of benzene was added 1 mL of [^{15}N]$PhNO_2$. The solution was bubbled for 5 min with oxygen and then added to finely ground $Fe_2(CO)_9$ (630 mg, 1.7 mmol) (Alfa, Ward Hill, MA) in a 50 mL round-bottomed flask equipped with a stirring bar. A mineral oil bubbler was attached to the flask and the evolution of CO_2 monitored as the orange suspension was vigorously stirred. When the bubbling stopped (∼4 h), the dark brown solution was diluted with methanol (20 mL) and then filtered to yield a brown paste. This paste was resuspended in methanol (30 mL), shaken, and then allowed to settle. The brown supernatant solution was removed, and the solid was washed in this way three more times. The golden powder remaining was filtered and dried with ether (192 mg, 23%). Anal. Calcd for $C_{18}H_{10}Fe_2N_2O_8$: C, 43.77; H, 2.04; N, 5.67. Found: C, 42.50; H, 2.01; N, 5.36.

Table 1. Experimental ^{15}N NMR Shifts and Shift Tensor Elements for Nitrosoarenes and Nitrosoarene Complexes

compound	δ_{iso} (ppm)[a]	δ_{11} (ppm)	δ_{22} (ppm)	δ_{33} (ppm)
1	802	1692	537	175
1·HCl	429	747	394	146
$ZnCl_2$(**1**)$_2$	583	1165	445	141
$SnCl_2Me_2$(**1**)$_2$	596	1174	472	145
$PdCl_2(PhNO)_2$	599	1137	508	153
$PdCl_2$(**1**)$_2$, site 1	473	839	460	130
$PdCl_2$(**1**)$_2$, site 2	459	794	453	127
$[Fe(CO)_3(PhNO)]_2$	171	286	144	82

[a] Referenced to NH_3 using solid NH_4Cl at 37.0 ppm.

Myoglobin−[^{15}N]Nitrosobenzene and Hemoglobin−[^{15}N]Nitrosobenzene. Adult human hemoglobin and horse heart myoglobin were both obtained from Sigma (Sigma-Aldrich, Inc., St. Louis, MO). The [^{15}N]nitrosobenzene adducts were prepared via reduction of the ferric protein with 1 equiv of [^{15}N]phenylhydroxylamine, prepared via reduction of [^{15}N]nitrobenzene with zinc, according to Mansuy et al.[24] The dilute protein solutions were concentrated via Amicon filtration. The isotropic solution ^{15}N NMR chemical shift of free PhNHOH is 117 ppm from $NH_{3(l,ext)}$, and was also evident in the protein spectra.

NMR Spectroscopy. Solid-state $^{15}N\{^1H\}$ cross-polarization (CP) magic-angle sample spinning (MAS) NMR spectra were recorded using "home-built" spectrometers which consist of 8.45 T, 3.5 in. bore and 11.7 T, 2.0 in. bore superconducting solenoid magnets (Oxford Instruments, Osney Mead, Oxford, U.K.), and Tecmag (Houston, TX) Aries and Libra data systems, together with a variety of other digital and rf circuitries. For rf pulse amplification, we used Amplifier Research (Souderton, PA) and Henry Radio (Los Angeles, CA) transmitters. Solid-state spectra were obtained by using 5 mm Doty Scientific (Columbia, SC) "magic-angle" sample-spinning (MAS) NMR probes. The 90° pulse widths varied from 4.6 to 12 μs. Solution spectra were recorded on a 600 MHz Varian (Mountain View, CA) Inova spectrometer, using 10 mm sample tubes. Chemical shifts for the solid state work were referenced indirectly to $NH_{3(l,ext)}$ using solid [^{15}N]NH_4Cl, taken to be 37 ppm downfield from $NH_{3(l,ext)}$.[46] These chemical shifts were also cross-referenced to the shift of liquid [^{15}N]CH_3NO_2 (381.7 ppm from NH_3) and 1 M [$^{15}N_2$]urea in DMSO (77 ppm downfield from NH_3).[46,47]

Tensor Determinations. Chemical shift tensor elements were determined from multiple slow-spinning-speed MAS NMR spectra using the Herzfeld−Berger method.[48] Typically, three spectra obtained at spinning frequencies from 1 to 5 kHz were analyzed by using a program kindly provided by Professor R. Wasylishen. The resulting tensor elements were then averaged, and the mean values are reported in Table 1. The errors vary, depending on the overall span of the tensor, and are thought to range from ∼5 to 20 ppm.

Shielding Calculations. The principal elements of the ^{15}N chemical shielding tensor and their orientations were computed using a density functional theoretical (DFT) method with the deMon program[49] kindly provided by Professor Dennis Salahub. Calculations were carried out on a cluster of International Business Machines (Austin, TX) RISC workstations, RS/6000 Models 340, 350, 360, 365, and 3CT. We used

(35) Overholser, P. G.; Yoe, J. H. *J. Am. Chem. Soc.* **1941**, *63*, 3224−3229.
(36) Popp, C. J.; Ragsdale, R. O. *Inorg. Chem.* **1968**, *7*, 1845−1848; Sutton, L. E. *Trans. Faraday Soc.* **1934**, *30*, 796−801.
(37) Cameron, M.; Gowenlock, B. G.; Vasapollo, G. *J. Organomet. Chem.* **1989**, *378*, 493−496.
(38) Cameron, M.; Gowenlock, B. G. *Polyhedron* **1994**, *13*, 1371−1377.
(39) Furniss, B. S.; Hannaford, A. J.; Smith, P. W. G.; Tatchell, A. R. *Vogel's Textbook of Practical Organic Chemistry;* Longman: Burnt Mill, England, 1989; p 911.
(40) Hu, S.; Thompson, D. M.; Ikekwere, P. O.; Barton, R. J.; Johnson, K. E.; Robertson, B. E. *Inorg. Chem.* **1989**, *28*, 4552−4554.
(41) Matsubayashi, G.-E.; Nakatsu, K. *Inorg. Chim. Acta* **1982**, *64*, L163−L164.
(42) Furniss, B. S.; Hannaford, A. J.; Smith, P. W. G.; Tatchell, A. R. *Vogel's Textbook of Practical Organic Chemistry*; Longman: Burnt Mill, England, 1989; p 956.
(43) Kharasch, M. S.; Seyler, R. C.; Mayo, F. R. *J. Am. Chem. Soc.* **1938**, *60*, 882−4. Knieriem, B. Ph. D. Thesis, Göttingen, 1972.
(44) Balch, A. L.; Petridis, D. *Inorg. Chem.* **1969**, *8*, 2247−2252.
(45) Koerner von Gustorf, F.; Jun, J.-J. *Z. Naturforsch. B* **1965**, *20*, 521−523.
(46) Witanowski, M. *Nitrogen NMR*; Plenum Press: London, England, 1973.
(47) Wishart, D. S.; Bigam, C. G.; Yao, J.; Abildgaard, F.; Dyson, H. J.; Oldfield, E.; Markley, J. L.; Sykes, B. D. *J. Biomol. NMR* **1995**, *6*, 135−140.
(48) Herzfeld, J.; Berger, A. *J. Chem. Phys.* **1980**, *73*, 6021−6030.
(49) Malkin, V. G.; Malkina, O. L.; Casida, M. E.; Salahub, D. R. *J. Am. Chem. Soc.* **1994**, *116*, 5898−5908.

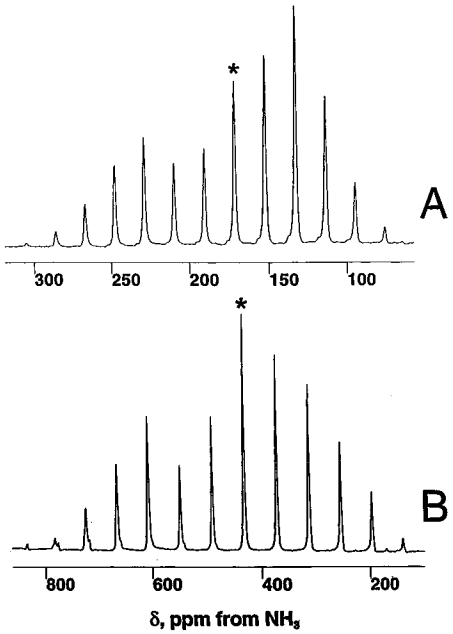

Figure 1. ^{15}N CP-MAS NMR (50.67 MHz) spectra of nitrosoarene systems: (A) $[Fe(CO)_3(PhNO)]_2$, 1,000 ± 2 Hz MAS rate, 15 ms mix, 60 s recycle, 2000 scans; (B) same as (A) but **1**·HCl, 3000 ± 2 Hz MAS rate. A line broadening of 15 Hz due to exponential multiplication was used in both cases. The asterisk indicates the isotropic shift.

a locally dense basis, iglo-iii[50] on the ^{15}N of interest, iglo-ii[50] on the other light atoms, and either an all electron representation for the metal or (for Pd) a model core potential.[49] A PW-91 functional and a fine grid[49] were employed in all calculations. For the dimeric iron compound, $[Fe(CO)_3(PhNO)]_2$, the X-ray structure is not known. We therefore used instead an analogous dimer structure, which contains 3-chloro-2-methylnitrosobenzene,[51] replacing the Cl and Me substituents with H for calculational purposes, since there is not expected to be any significant structural difference in M−NO bonding based on phenyl substituent differences.[27] Typical calculations took about 12 h on an IBM RS/6000 Model 365 system equipped with 64 Mbyte of memory and 4 Gbyte of disk space.

Results and Discussion

We obtained the magic-angle spinning ^{15}N NMR spectra of each of the ^{15}N-labeled compounds whose preparation was described above, at several spinning speeds, to deduce the principal components of the ^{15}N shielding tensor in different metal−ligand bonding environments. Two representative spectra are shown in Figure 1. The shift tensor elements are illustrated graphically in Figure 2 and are also tabulated in Table 1, together with the isotropic chemical shifts. From a purely experimental perspective, it is clear that the overall width of the shielding tensor is overwhelmingly dominated by the position of δ_{11}, the most downfield or least shielded tensor component, since the most shielded tensor component, δ_{33}, varies very little with metal or hydrogen ion addition.

The experimental shift tensor element trends are all very well reproduced from the DFT chemical shielding calculations, and we show in Figure 3 plots of the experimental isotropic shifts (minus the Sn data, discussed below) versus the theoretical isotropic shieldings, as well as the experimental shift tensor elements (δ_{ii}) versus the theoretical shielding tensor elements (σ_{ii}). For the isotropic shifts, we obtain a slope of −0.91 and an R^2 value of 0.94, to be compared with the ideal results of

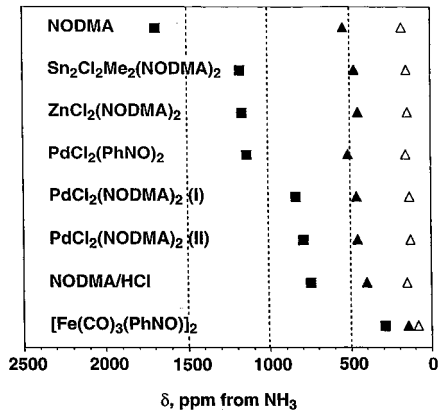

Figure 2. Experimental values for the nitrogen-15 shielding tensor elements in the systems investigated: (■) δ_{11}, (▲) δ_{22}, (△) δ_{33}.

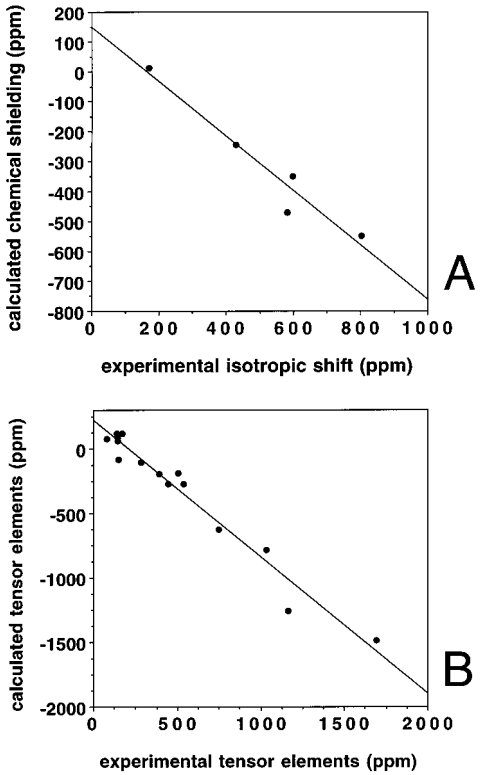

Figure 3. Experimental versus theoretical nitrogen-15 chemical shift and shielding tensor results: (A) isotropic shifts, slope = −0.91, R^2 = 0.943; (B) shift tensor elements, slope = −1.03, R^2 = 0.966. The result for the Sn complex has been omitted. See the text for details.

−1 and +1, while for the tensor elements we obtain a slope of −1.03 and an R^2 value of 0.97. The DFT method we have used has been shown previously to account in an effective manner for the effects of electron correlation and exchange,[49] with excellent results being obtained on other organometallic systems, such as metal carbonyls[52] and olefin complexes.[53] In earlier work on nitroso compounds at the Hartree−Fock level, the shielding was underestimated,[26] and it was pointed out there that correlation effects would be expected to be quite important, especially for free *p*-$NOC_6H_4NMe_2$, due to the low-lying excited states in the nitrosoarenes.

In addition to these studies of simple model M−RNO complexes, we have also investigated the ^{15}N shielding of [^{15}N]-

(50) Kutzelnigg, W.; Fleischer, U.; Schindler, M. *NMR Basic Principles and Progress*; Springer-Verlag: New York, 1991; Vol. 23, pp 165−262.
(51) Barrow, M. J.; Mills, O. S. *J. Chem. Soc. A* **1971**, 864−868.
(52) Kaupp, M. *Chem. Eur. J.* **1996**, *2*, 348−357.
(53) Havlin, R. H.; McMahon, M.; Srinivasan, R.; Le, H.; Oldfield, E. *J. Phys. Chem., A* **1997**, *101*, 8908−8913.

Table 2. Calculated ^{15}N Shielding Tensor Elements and Isotropic Shieldings, Orientation of ^{15}N Shielding Tensor Elements, and Calculated Mayer Bond Orders for Nitrosoarenes and Related Systems

compound	δ_{iso} (ppm)[a]	σ_{iso} (ppm)	σ_{11} (ppm)	σ_{22} (ppm)	σ_{33} (ppm)	α (deg)[b]	β (deg)[c]	NO bond order
1	791	−546	−1488	−268	118	19.2	90.9	1.650
1·HCl	489	−244	−625	−190	84	25.9	90.0	1.104
$ZnCl_2(\mathbf{1})_2$	545	−300	−873	−153	127	31.0	87.0	1.410
$SnCl_2Me_2(\mathbf{1})_2$	890	−645	−1776	−268	110	75.4	16.9	1.548
$PdCl_2(PhNO)_2$	602	−357	−800	−190	−81	34.4	89.9	1.262
$[Fe(CO)_3(PhNO)]_2$	218	27	−84	74	91	44.0	80.1	0.954
PhNO	841	−596	−1671	−216	99	67.5	90.9	1.780
PhNO−heme model	641	−396	−1042	−234	90	29.0	89.6	1.541

[a] $\delta(NH_3) = 244.6 - \sigma$. [b] Angle between σ_{11} and the N−O bond axis. [c] Angle between σ_{33} and the C−NO plane.

PhNO bonded to the iron atom in myoglobin from horse heart (Mb), and adult human hemoglobin (Hb). For myoglobin, there is (as expected) a single resonance, resonating at 562 ppm downfield from $NH_{3(l,ext)}$, while in Hb·PhNO there is also one peak, at 580 ppm. To calculate the isotropic (and anisotropic) shieldings of these heme proteins, we have used as an initial structure the (imidazole)(bisamidinato)iron(II) heme model used previously by several other groups:[54−56]

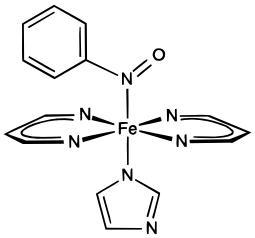

We used bond lengths and bond angles based on a crystallographic study of the 2-nitrosopropane adduct of Fe−tetraphenylporphyrin,[19] the isotropic chemical shift being predicted using the absolute shielding of NH_3,[57] $\delta(ppm) = 244.6 - \sigma$. For the PhNO heme model calculation, we obtain an isotropic shift of 641 ppm, in moderate accord with the experimental shifts of 562 ppm downfield from $NH_{3(l,ext)}$ obtained for Mb·PhNO and 580 ppm for adult human hemoglobin.

The only compound which does not fit the correlation between the experimental and theoretical values is $SnCl_2Me_2(p\text{-}NOC_6H_4NMe_2)_2$. However, on close inspection of the X-ray structure[41] it can be seen that the N−O bond length is very short, only 1.218 Å. In fact, this N−O bond length is, according to the published structure, even shorter than that found in an uncoordinated nitroso compound.[34]

A search of the Cambridge Crystallographic Database revealed that while it is possible to have N−O bond lengths of this magnitude in M−N-coordinated systems, there are no other known oxygen-coordinated systems having N−O bond lengths below ∼1.3 Å. On the basis of this result, which represents about a 0.1 Å deviation in bond length in the X-ray study and the only major outlier in the chemical shift calculations, we conclude that the N−O bond length in $SnCl_2Me_2(p\text{-}NOC_6H_4NMe_2)$ is most likely much longer, probably close to the 1.305 Å seen in $ZnCl_2(p\text{-}NOC_6H_4NMe_2)_2$.[40]

For the hydrochloride salt of $p\text{-}NOC_6H_4NMe_2$, there is some question as to the actual site of protonation, and this can be expected to influence the calculations in a major way. Is the hydrochloride protonated on the nitroso nitrogen or the amine nitrogen? In previous work, the proton NMR spectrum of **1** in CF_3COOH has been shown to consist of only one singlet for the *N*-methyl group.[33,36] This suggests that the oxygen is protonated; however, because of the relatively broad lines, there is still some uncertainty,[35] and in the X-ray structure,[58] the position of the proton in the hydrochloride salt was not detectable using a difference Fourier map. It was suggested, however, that on the basis of the long N−O bond length (1.374 Å), compared to 1.243 Å in unprotonated **1**, together with the relatively long bond lengths in the phenyl ring (implying a quinonoid structure), protonation occurs on oxygen.

A more direct approach to detecting sites of protonation is to use ^{15}N NMR and quantum chemistry. Here, we simply calculate the ^{15}NO shifts for both the N- and O-protonated species. Experimentally, we obtain $\delta_i = 429$ ppm and $\Delta\sigma = |\sigma_{33} - \sigma_{11}| = 601$ ppm (Table 1). Theoretically, we obtain $\delta_i = 453$ ppm and $\Delta\sigma = 709$ ppm for the O-protonated species, but $\delta_i = 1082$ ppm and $\Delta\sigma = 2471$ ppm for the N-protonated species. Clearly, the hydrochloride salt is protonated on oxygen, consistent with the conclusions drawn indirectly from the X-ray study.[58]

Shielding Tensors and Bonding. We now consider in more detail the actual magnitudes and orientations of the shielding tensor elements we have observed and calculated, together with some structural and bonding correlations which can be deduced from these results. Previously, Wasylishen et al. reported the magnitude and in one case the orientation of several ^{15}N shielding tensors in nitrosoarenes and related compounds.[26] On the basis of theory and experiment, they found that the most shielded component, δ_{33}, was more or less perpendicular to the R−N═X plane and that δ_{22} is approximately oriented along the nitrogen lone pair, while the most deshielded component, δ_{11}, is close to the N═X bond axis. The large deshielding of δ_{11} was attributed to low-lying $n_N \rightarrow \pi^*$ transitions, with δ_{11} oriented close to the N═X bond axis, while the most shielded component, δ_{33}, was influenced by high-energy in-plane circulations, due to $\sigma \rightarrow \sigma^*$ transitions.[26] In addition to investigating **1**, these workers also studied the ^{15}N shielding tensors in the *cis*-nitrosobenzene dimer, **2**, and three related molecules: *trans*-azobenzene, **3**; benzylideneaniline, **4**; and (*E*)-acetophenone oxime, **5** Interestingly, for all of these compounds, the orientations of the tensor components were not thought to vary very much, but the magnitudes of δ_{11} decreased in going from **2** to **5**. Since theoretical results for these compounds were not reported, but two possible orientations of the shielding tensor of **2** were determined experimentally, we therefore carried out calculations on **2**−**5** to determine, first, the principal elements of the shielding tensors and, second, their orientations, which

(54) Jewsbury, P.; Yamamoto, S.; Minato, T.; Saito, M.; Kitagawa, T. *J. Am. Chem. Soc.* **1994**, *116*, 11586−11589.
(55) Strich, A.; Veillard, A. *Theor. Chim. Acta* **1981**, *60*, 379−383.
(56) Newton, J. E.; Hall, M. B. *Inorg. Chem.* **1984**, *23*, 4627−4632.
(57) Jameson, C. J.; Jameson, A. K.; Oppusunggu, D.; Willie, S.; Burrell, M.; Mason, J. *J. Chem. Phys.* **1981**, *74*, 81−88.
(58) Drangfelt, O.; Rømming, C. *Acta Chem. Scand. A* **1974**, *28*, 1101−1105.

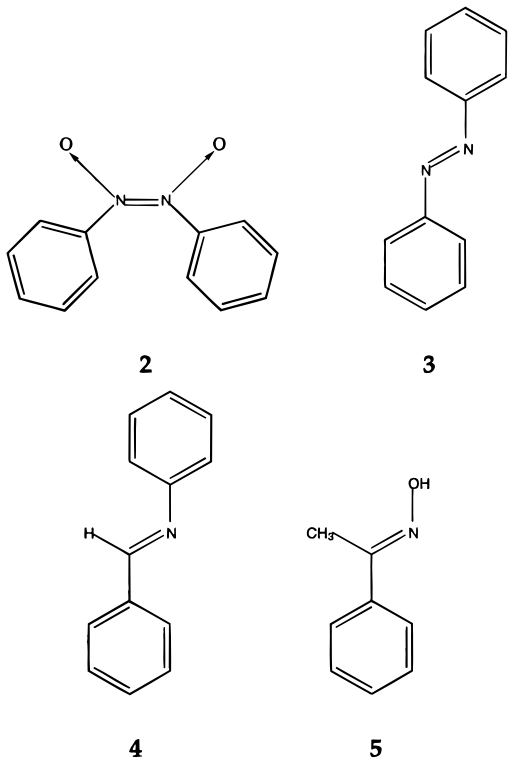

2 **3** **4** **5**

for **2** can be compared with the experimental results.[26] We show in Table 3 the results obtained theoretically, which are then compared with the 12 experimental shielding tensor elements in Figure 4. We find a slope = −0.91 and an R^2 value of 0.943, indicating good accord with experiment. We also show graphically in Figure 5 the actual orientation of the tensor. There is good agreement between theory and experiment, not only for the magnitudes of the tensor elements and the absolute shielding (Table 3) but also for the orientation, with σ_{11} being clearly oriented close to the C−N bond axis, in accord with the results of Lumsden et al.[26]

We now consider in more detail the orientations of the shielding tensors for the nitrosoarene−metal complexes we have investigated, including in many cases correlations with structural parameters, such as bond lengths and bond order.

The δ_{11} and δ_{22} components of the shielding tensor are in or close to the R−N═O plane, while δ_{33} is approximately perpendicular to it, as shown below. More quantitatively, we follow Wasylishen et al.[26] and define an angle, α, between the most deshielded tensor element, δ_{11}, and the N═O bond axis and an angle, β, between the most shielded component, δ_{33}, and the R−N═O plane:

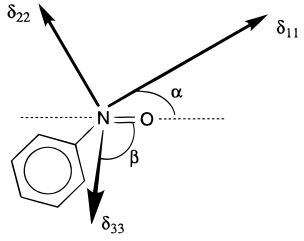

We present results for α and β in Table 2. This orientation of the three tensor elements is reminiscent of that found in other isoelectronic ligand systems, such as olefins.[53] This simple picture begins to break down in more complex bonding situations, for example, in the nitrosobenzene−iron dimer, where

Table 3. Computed ^{15}N Shielding Tensor Elements for Model Systems

compound	σ_{11} (ppm)	σ_{22} (ppm)	σ_{33} (ppm)	σ_{iso} (ppm)
cis-nitrosobenzene dimer (**2**) (two sites)	−227	−24	44	−69
	−229	−18	46	−67
trans-azobenzene (**3**) (two sites)	−741	−163	157	−249
	−743	−164	157	−250
benzylidene aniline (**4**)	−379	−106	178	−102
(*E*)-acetophenone oxime (**5**)	−351	−106	67	−130

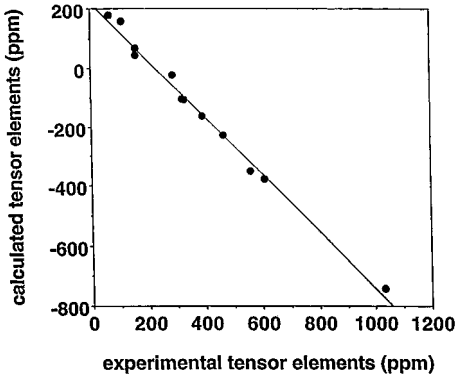

Figure 4. Correlation between the experimental shift and calculated shielding tensor elements for compounds **2**−**5** (slope = −0.91, R^2 = 0.943).

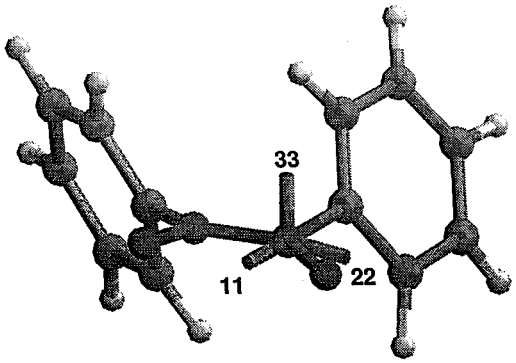

Figure 5. Tensor orientation for compound **2** computed using the deMon DFT approach.

N is bonded to two iron atoms and O to one iron atom, which results in a larger deviation (∼10°) of δ_{33} from the PhNO normal:

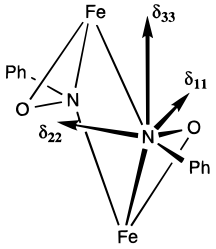

The central component of the tensor, δ_{22}, is oriented in each case close to the lone pair of the nitrogen. For the metal adducts of **1**, we also note that as the O−N−C (phenyl) angle increases, δ_{22} increases, while α decreases as shown in Figure 6. There is a significant difference in this trend when the ligand changes from **1** to nitrosobenzene, implying a large contribution of the quinonoid resonance structure to shielding in the former ligand system.

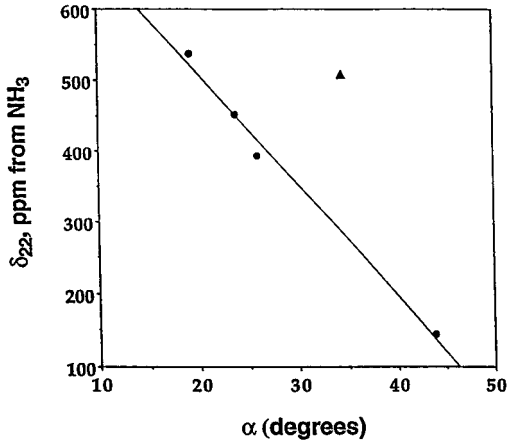

Figure 6. Correlation between the experimental tensor components, δ_{22}, and the corresponding angles, α. The solid dots indicate NODMA compounds and the Fe−PhNO dimer, while the triangle represents the palladium−PhNO complex.

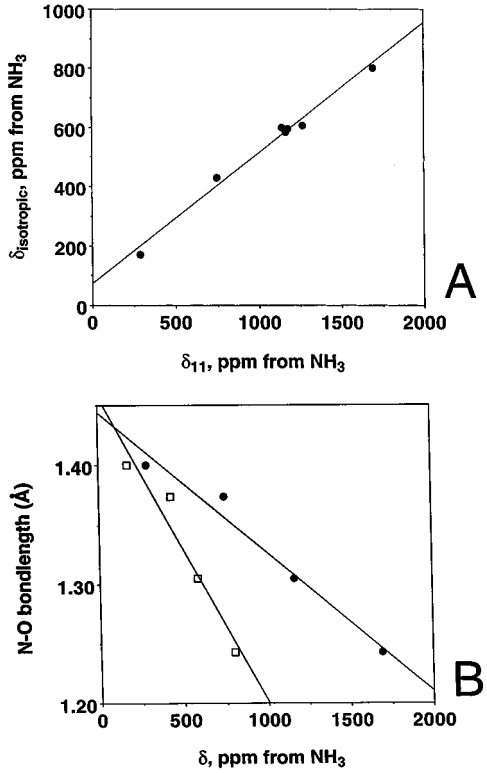

Figure 7. Tensor element, isotropic shift, and bond length correlations: (A) correlation between the most deshielded tensor element, δ_{11}, and the isotropic shift, showing that the tensor is dominated by δ_{11}; (B) graph showing the dependence of the isotropic shift and δ_{11} on the N−O bond lengths. R^2 values: (□) = 0.990 (isotropic shift); (●) 0.971 (δ_{11}). The Sn and Pd−PhNO compounds are omitted. See the text for details.

The component which changes most dramatically from one compound to another is the most deshielded one, δ_{11}, and as can be seen in Figure 7A, it is the behavior of δ_{11} which overwhelmingly dominates the observed changes in isotropic shift from compound to compound. Because of the relatively close proximity of this component to the N−O bond vector, the influence of the binding mode between RNO and the ligand, or more specifically whether N or O coordination is involved, can be expected to influence the $n_N \rightarrow \pi^*$ transition energy. Our results indicate a moderate correlation between the N−O bond length and the magnitude of δ_{11} for **1**, $ZnCl_2[p\text{-}NOC_6H_4\text{-}NMe_2]_2$, **1**·HCl, and $[Fe(CO)_3(PhNO)]_2$ (Figure 7B). However, $PdCl_2(PhNO)_2$ is off of the trend. Therefore, the simple idea of having a reliable method with which to determine the N−O bond length from the tensor element, δ_{11}, fails. Of course, it would be surprising if such a general relationship between shielding and bond length or tensor orientation were found in such a range of bonding situations, involving different metal ions as ligands. However, interesting trends are clearly apparent (Figures 7 and 8), and it is possible that such correlations may find future use when more similar ligands or metal groups are investigated.

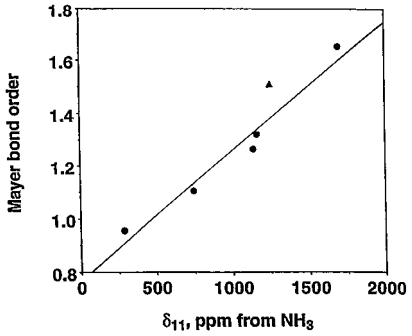

Figure 8. Correlation between Mayer bond order and δ_{11} for NODMA compounds ($R^2 = 0.963$) (triangle indicates calculated δ_{11} for the heme protein−PhNO complex).

Perhaps then, a more likely candidate for a structural correlation would be the bond order in the nitroso group, since this should be related to the $n_N \rightarrow \pi^*$ excitation energy. We therefore determined the Mayer bond orders for each of the compounds investigated, and the results are given in Table 2 and Figure 8. There is an excellent correlation using either δ_{11}, which we have shown dominates the shielding trends seen in the nitrosoarenes, or the bond order. In the case of **1**, the calculated NO bond order is 1.650, which correlates with the large deshielding observed experimentally:

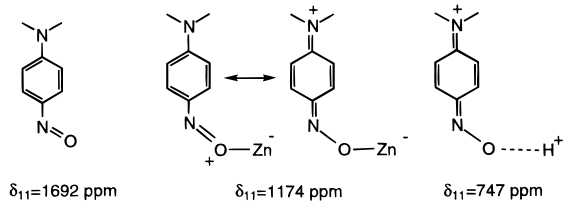

For the Zn complex, the bond order decreases to 1.410, consistent with the increased shielding, while in the case of **1**·HCl, the bond order decreases to only 1.104, which correlates well with the observed highly shielded 747 ppm chemical shift observed for δ_{11}, as illustrated above and in Figure 8. In the case of the quinonoid structure, **1**·HCl, there is essentially no double bond character between N and O, so the $n_N \rightarrow \pi^*$ transition energy increases considerably, as also evidenced by the dramatic color change seen on protonation. Similarly, for $[Fe(CO)_3(PhNO)]_2$, where the nitrosobenzene acts as a bridging ligand, we have formally only a single N−O bond, with both N and O being coordinated to iron. The calculated bond order is 0.954, and δ_{11} decreases to 286 ppm, while all other experimental δ_{11} values in metal complexes are in the range 747−1692 ppm (Table 1).

The trends we have seen so far for δ_{iso} do not permit a ready differentiation between N and O ligation. Our results do suggest, however, that δ_{11} becomes more shielded when nitrogen is the ligand atom, because in this case the lone pair is more localized in the metal−ligand bond. In the case of oxygen

as the metal ligand, there is still partial NO double-bond character, and the lone pair on nitrogen is available for $n_N \rightarrow \pi^*$ donation. This effect appears important from the perspective of understanding metal−ligand bonding in hemoglobin and myoglobin, and the general trend we are proposing is clearly apparent in the series PhNO → model heme·PhNO → $(PhNO)_2$:

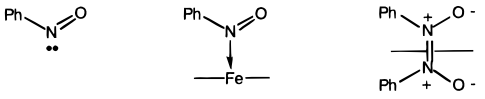

In PhNO, our calculations indicate that σ_{11} increases from −1671 to −1042 ppm on binding to iron, close to the value of −800 ppm found in $PdCl_2(PhNO)_2$ (Table 2). However, for σ_{22} and σ_{33}, we find very similar results between free and heme-bound PhNO: $\sigma_{22} = -216$ (free), −234 (bound) ppm, and $\sigma_{33} = 99$ (free), 90 (bound) ppm, consistent with the above idea. In the most extreme case of essentially no NO double-bond character, the lone pair is no longer available and we find extreme shielding, $\sigma_{11} \sim -200$ ppm for *cis*-$(PhNO)_2$ (Tables 2 and 3). These results are consistent with the involvement of the nitrogen lone pair in metal bonding in the heme model system.

Similar arguments may also help explain qualitatively the differences in δ_{11} between the $PdCl_2(p\text{-}NOC_6H_5)_2$ and $PdCl_2(p\text{-}NOC_6H_4NMe_2)_2$ complexes. In the case of nitrosobenzene, there is strictly an N═O double bond, whereas with the NMe_2 derivative, the quinonoid resonance results in reduced double-bond character in the NO group. This leads to a more shielded δ_{11} value for the $PdCl_2$ complexes with **1** compared with the nitrosobenzene complexes:

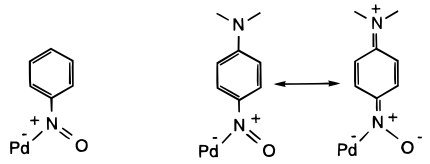

Our results also indicate that there is a good correlation between the experimental δ_{11} values and the calculated Mayer bond orders, independent of whether nitrosobenzene or **1** is used, in a range of metal−RNO complexes. For the heme proteins, the *computed* δ_{11} also fits this correlation (Figure 8). We find a bond order of 1.54 from calculation, to be compared with a predicted value based on the isotropic chemical shift of 1.52.

Finally, we also carried out an investigation of the localized molecular orbital contributions to shielding for each of the systems studied.[50,52] In such complex systems, there are numerous contributions to shielding. We therefore simplified the situation and defined three major regions, A, B, and C:

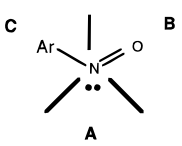

The A region, containing the N lone pair and whatever associated ligands were attached (e.g., Zn, Cl) showed a clear dominance on shielding, while the B and C contributions were, in general, relatively constant from one compound to another. As expected, the A effects were largest for σ_{11}, which as noted above clearly dominates the shielding trends seen experimentally.

In the future, it may also be possible to investigate additional NMR spectroscopic probes, such as the ^{17}O shielding and efg, in such systems. However, the electric field gradient is expected to be quite large for such complexes, making solid-state measurements difficult. It might also be thought that ^{14}N NMR or ^{14}N efg experiments could also be useful structural probes. This is likewise a difficult problem, since in MeNO we find an ^{14}N quadrupole coupling constant of ~ -5.4 MHz, making detection rather difficult in model systems, and not at all feasible in proteins, unlike ^{15}N NMR. However, for heme proteins and model systems, both ^{57}Fe NMR shifts and Mössbauer quadrupole splittings are now becoming calculable, and should be a valuable complement to ligand shieldings.

Conclusions

The results we have presented above are interesting for several reasons. First, they represent the first experimental determination of the solid-state ^{15}N NMR chemical shielding tensors for nitrosoarenes in a wide range of metal−ligand bonding situations. Second, the results of density functional calculations permit the first accurate predictions of [^{15}N]nitrosoarene shielding tensors, with slope and R^2 values being within 5−10% of the ideal values. Third, our results represent the first DFT predictions of the orientations of the principal components of the ^{15}N shielding tensor in a series of RNO·metal and model systems, with good agreement between theory and experiment in the case of dioxyazodibenzene. Fourth, our results show that the protonation site in *p*-nitroso-*N*,*N*-dimethylaniline can be determined by using solid-state NMR and quantum chemistry. Fifth, our results indicate that strong evidence can be found for N versus O coordination, from an analysis of the ^{15}N shielding tensors, although exceptions can be found. Sixth, our results demonstrate the first observation of the ^{15}N chemical shifts in PhNO bound to both hemoglobin and myoglobin, with the observed shifts being predicted via DFT methods with reasonable accuracy, and N coordination being implied. Seventh, we have found a number of interesting correlations among bond lengths, bond orders, and shift/shielding tensor elements, which appear to be of use in understanding some aspects of metal−ligand bonding and shielding in these systems.

Acknowledgment. We thank Professor Dennis Salahub and Drs. V. Malkin, O. Malkina, and E. Proynov for providing their deMon program. We are also grateful to a reviewer for his constructive comments. This work was supported by the United States Public Health Service (National Institutes of Health Grant HL-19481).

JA971587T